Taming spatial dispersion in wire metamaterial

2008 J. Phys.: Condens. Matter 20 295222

(http://iopscience.iop.org/0953-8984/20/29/295222)

J. Phys.: Condens. Matter **20** (2008) 295222 (11pp) doi:10.1088/0953-8984/20/29/295222

Taming spatial dispersion in wire metamaterial

A Demetriadou and J B Pendry

The Blackett Laboratory, Imperial College London, SW7 2AZ, UK

E-mail: ademetri@imperial.ac.uk and j.pendry@imperial.ac.uk

Received 20 December 2007, in final form 12 June 2008
Published 1 July 2008
Online at stacks.iop.org/JPhysCM/20/295222

Abstract

Thin wire structures are commonly used as 'metamaterials' for simulating the negative electrical response of a plasma. In this they are only partially successful: transverse modes are convincingly reproduced but problems arise from highly dispersive longitudinal modes which can be excited by externally incident radiation and impair the validity of the simple local plasma model. We show how modified designs can essentially eliminate the longitudinal dispersion and restore the simple local model.

(Some figures in this article are in colour only in the electronic version)

1. Introduction

Electromagnetic properties of homogeneous materials are described by the electrical permittivity, ε, and magnetic permeability, μ. This description admits anisotropic materials in which case ε and μ are tensor quantities, and also dispersion when one or both of ε and μ may depend on frequency. The electric and magnetic fields concerned are recognized to be averages over their microscopic values. Recently this description has been extended to a new class of materials, metamaterials, where the microscopic structure is on a larger scale than the atomic. If the microstructure is much less than a wavelength in scale we can still speak of a local average for fields and a description in terms of ε and μ may again be appropriate. Creating novel electromagnetic properties through structured media gives access to a whole new range of phenomena. Prominent amongst these is negative refraction which as Veselago predicted [1] is realized when both electric and magnetic responses are negative:

$$\varepsilon < 0, \qquad \mu < 0. \tag{1}$$

At microwave frequencies, structured media, otherwise known as metamaterials, are generally deployed to achieve this condition.

The electron plasma in a metal typically has a response of the form [2, 3],

$$\varepsilon = 1 - \frac{\omega_{\mathrm{p}}^2}{\omega(\omega + \mathrm{i}\gamma)} \tag{2}$$

where ω_{p} is the natural resonant frequency of the electron gas, γ represents resistive losses in the system and ω is the frequency of the wave. We can express ω_{p} in terms of the electron density, n, the electronic charge, e, and mass, m_e [3],

$$\omega_{\mathrm{p}}^2 = \frac{ne^2}{\varepsilon_0 m_e} = (c_0 k_{\mathrm{p}})^2 \tag{3}$$

where k_{p} is the wavevector corresponding to ω_{p}. For typical metals ω_{p} lies in the optical or UV region of the spectrum. Figure 1 shows in dotted and dashed lines the resulting dispersion for transverse and longitudinal modes respectively, for an electron plasma in a metal.

To create a negative electric response at microwave frequencies, an artificial plasma is created from a wire structure [2–8] in which all dimensions are less than the wavelength. A typical wire structure is shown in figure 2(a), where thin connected wires, of radius r, are placed in a cubic lattice with periodicity a (i.e. the lattice constant). The wires are along the three orthogonal axes and the radius of the wires is much smaller than the periodicity (i.e. $r \ll a$). The wires leave electrons free to move whilst reducing their effective density. Also thin wires possess a large inductance which acts like an effective mass. Equation (3) then predicts a considerable reduction in the plasma frequency. Ideally these structures can be modelled by a local effective dielectric response of conventional plasma form, shown in (2), but in practice complications arise.

The simple analysis leading to equation (2) is valid when the electric field is parallel to one of the three sets of wires, but it has been shown that important corrections are needed when the field is not parallel to the wires [9]. These corrections spoil the simple picture of a local medium and replace it with a

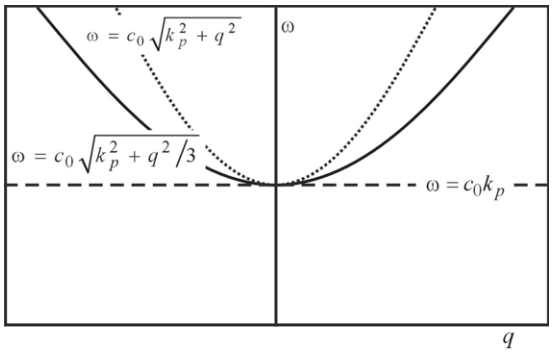

Figure 1. Dispersion of radiation in a plasma. In the ideal case two degenerate transverse modes (dotted line) disperse as $\omega = c_0\sqrt{k_\mathrm{p}^2 + q^2}$ where $k_\mathrm{p} = \omega_\mathrm{p}/c_0$ (i.e. the wavevector corresponding to the plasma frequency) and in addition there is a dispersionless longitudinal mode (dashed line), $\omega = c_0 k_\mathrm{p} = \omega_\mathrm{p}$. In wire structures designed to imitate an ideal plasma the longitudinal mode (full line) is dispersive: $\omega = c_0\sqrt{k_\mathrm{p}^2 + q^2/3}$, where q is the wavevector in the structure.

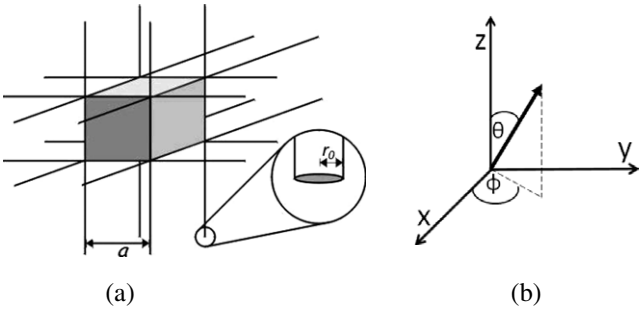

Figure 2. (a) A lattice of metallic wires mimics the properties of a true plasma provided that the lattice constant, a, is much less than the wavelength of incident radiation. Note that in this example the wires are joined at the nodes, where r_0 is the radius of the wires and a the lattice constant. (b) The wires are aligned with the three orthogonal axes and the translation from orthogonal to spherical coordinates is shown, where θ and ϕ angles are shown.

more complex picture in which the dielectric response depends strongly on the wavevector, i.e. the medium is non-local. The dispersion of the longitudinal mode is shown in figure 1 with the full line. This renders the wire structures much less useful as metamaterials, because of the resulting complex response to incident fields.

In this paper, first we present a simple argument that reproduces the results of earlier work and identifies the source of the problem, and then go on to propose modifications to the wire structure that minimize the dispersion and result in an effectively local dielectric response.

As we shall show, the problem lies in the very small capacitance of the wires, which comes into play whenever charge accumulates on the wires. For a transverse wave with electric fields parallel to the wires no charge accumulates and the wire capacitance is irrelevant, hence (2) provides a satisfactory description. If the three sets of wires shown in figure 2(a) are not joined at the nodes a problem arises as soon as the electric fields stray from the parallel case, because then the currents flowing would be required to leap from one wire to the next and the lack of capacitative coupling, strongly inhibits this flow. A true plasma in which electrons are free to move in any direction does not suffer from this limitation. Hence the extreme non-locality found in disconnected systems.

Joining wires at the nodes fixes this particular problem, but others remain. Implicit in equation (2) is the assumption that there exists a longitudinal mode (the bulk plasmon) that is degenerate for all wavevectors and to a good approximation this is true for the electron plasma in a metal. A longitudinal mode implies periodic accumulation of charge resulting from the non-zero divergence of the electric field,

$$\nabla \cdot \boldsymbol{E}\exp(\mathrm{i}\boldsymbol{q}\cdot\boldsymbol{r} - \mathrm{i}\omega t) = \boldsymbol{q}\cdot\boldsymbol{E}_0\exp(\mathrm{i}\boldsymbol{q}\cdot\boldsymbol{r} - \mathrm{i}\omega t) \neq 0 \quad (4)$$

where $\boldsymbol{E}$ and $\boldsymbol{q}$ are the electric field and the wavevector in the wire metamaterial, respectively. Evidently the bigger $\boldsymbol{q}$ gets the more charge there is. In the wire structures this charge has to be parked on the wires which due to their low capacitance costs a lot of energy and in turn forces up the frequency with increasing $\boldsymbol{q}$. In a wire structure, far from showing no dispersion, longitudinal modes are highly dispersive implying strong non-locality of the system and invalidating (2). Longitudinal modes cannot be excited if the permittivity is independent of $\boldsymbol{q}$. This necessarily implies that the frequency of the longitudinal mode (ω_L) is independent of $\boldsymbol{q}$ and $\varepsilon(\omega_\mathrm{L}) = 0$ (i.e. the propagation velocity is zero-$\mathrm{v}_g = \mathrm{d}\omega_\mathrm{L}/\mathrm{d}\boldsymbol{q} = 0$). Dispersion introduces the complication that both longitudinal and transverse modes can be excited and convey energy into the material.

We show that there are two ways to fix this problem. Either we can increase the capacitance of the wires, for example by adding plates to the structure, thus minimizing dispersion. Alternatively we can increase the inductance of the wires which reduces the ratio of capacitative to inductive impedance. Both these approaches greatly minimize the dispersion of the longitudinal mode and lead to a material in which a simple local expression accurately describes the response to incident radiation.

2. Thin connected wires in 3D

Consider a lattice of wires arranged in a simple cubic $a \times a \times a$ pattern shown in figure 2(a). We seek self-consistent solutions of Maxwell's equations where the currents in the wires support the surrounding field. The current flowing in a wire oriented in the x- direction and located at lattice point YZ, is:

$$I\hat{\boldsymbol{x}}\sin\theta\cos\phi\exp(\mathrm{i}q_x x + \mathrm{i}q_y Y + \mathrm{i}q_z Z - \mathrm{i}\omega t) \quad (5)$$

where θ and ϕ are shown in figure 2(b) and Y, Z are the coordinates of the wire in question in the y–z plane. Corresponding expressions hold for the other two sets of wires. As a first approximation, to be corrected later, we average the current density over the three sets of wires,

$$\begin{aligned}\boldsymbol{j}' &= Ia^{-2}(\hat{\boldsymbol{x}}\sin\theta\cos\phi + \hat{\boldsymbol{y}}\sin\theta\sin\phi + \hat{\boldsymbol{z}}\cos\theta)\\ &\quad\times\exp(\mathrm{i}q_x x + \mathrm{i}q_y y + \mathrm{i}q_z z - \mathrm{i}\omega t)\\ &= \boldsymbol{j}_0 a^{-2}\exp(\mathrm{i}q_x x + \mathrm{i}q_y y + \mathrm{i}q_z z - \mathrm{i}\omega t) \quad (6)\end{aligned}$$

where,

$$\boldsymbol{j}_0 = I(\hat{\boldsymbol{x}}\sin\theta\cos\phi + \hat{\boldsymbol{y}}\sin\theta\sin\phi + \hat{\boldsymbol{z}}\cos\theta) \tag{7}$$

and the average charge is,

$$\rho' = \frac{\boldsymbol{j}_0\cdot\boldsymbol{q}}{a^2\omega}\exp(\mathrm{i}q_x x + \mathrm{i}q_y y + \mathrm{i}q_z z - \mathrm{i}\omega t). \tag{8}$$

From Maxwell equations:

$$\nabla\cdot\boldsymbol{E} = \rho'/\varepsilon_0 \qquad \text{and} \qquad \nabla\times\boldsymbol{B} - \frac{1}{c_0^2}\frac{\partial\boldsymbol{E}}{\partial t} = \mu_0\boldsymbol{j}' \tag{9}$$

and using the definition of vector potential $\boldsymbol{A}$ (i.e. $\boldsymbol{B} = \nabla\times\boldsymbol{A}$) and of scalar potential ϕ (i.e. $\boldsymbol{E} = -\frac{\partial\boldsymbol{A}}{\partial t} - \nabla\phi$) and by considering the gauge of $\boldsymbol{A}$ through Lorentz condition in free space (i.e. $\nabla\cdot\boldsymbol{A} + \frac{1}{c_0^2}\frac{\partial\phi}{\partial t} = 0$), two differential equations for $\boldsymbol{A}$ and ϕ emerge:

$$\nabla^2\boldsymbol{A} - \frac{1}{c_0^2}\frac{\partial^2\boldsymbol{A}}{\partial t^2} = -\mu_0\boldsymbol{j}' \tag{10}$$

$$\nabla^2\phi - \frac{1}{c_0^2}\frac{\partial^2\phi}{\partial t^2} = -\frac{\rho'}{\varepsilon_0} \tag{11}$$

which can be solved by assuming $\boldsymbol{A} = \boldsymbol{A}_0\exp(\mathrm{i}q_x x + \mathrm{i}q_y y + \mathrm{i}q_z z - \mathrm{i}\omega t)$ and $\phi = \phi_0\exp(\mathrm{i}q_x x + \mathrm{i}q_y y + \mathrm{i}q_z z - \mathrm{i}\omega t)$ and give the average fields of $\boldsymbol{A}$ and ϕ:

$$\begin{aligned}\boldsymbol{A} &= \frac{\mu_0\boldsymbol{j}_0}{(q^2-k_0^2)a^2}\exp(\mathrm{i}q_x x + \mathrm{i}q_y y + \mathrm{i}q_z z - \mathrm{i}\omega t)\\ \phi &= \frac{\boldsymbol{j}_0\cdot\boldsymbol{q}}{(q^2-k_0^2)\varepsilon_0\omega a^2}\exp(\mathrm{i}q_x x + \mathrm{i}q_y y + \mathrm{i}q_z z - \mathrm{i}\omega t).\end{aligned} \tag{12}$$

Hence,

$$\boldsymbol{B} = \mathrm{i}\boldsymbol{q}\times\boldsymbol{A} = \frac{\mathrm{i}\mu_0\mathbf{q}\times\mathbf{j}_0}{(q^2-k_0^2)a^2}\exp(\mathrm{i}q_x x + \mathrm{i}q_y y + \mathrm{i}q_z z - \mathrm{i}\omega t) \tag{13}$$

$$\boldsymbol{E} = \mathrm{i}\omega\boldsymbol{A} - \mathrm{i}\boldsymbol{q}\phi = \left[\mathrm{i}\omega\mu_0\boldsymbol{j}_0 - \mathrm{i}\boldsymbol{q}\frac{\boldsymbol{j}_0\cdot\boldsymbol{q}}{\varepsilon_0\omega}\right]\frac{1}{(q^2-k_0^2)a^2} \times \exp(\mathrm{i}q_x x + \mathrm{i}q_y y + \mathrm{i}q_z z - \mathrm{i}\omega t). \tag{14}$$

If we assume the wires to be perfect conductors, the parallel component of the field at the wires must be zero. For wires in, say, the x-direction comprise E_x, the smooth averaged contribution shown above in (14), and the local fluctuations which will be very strong close to the wire in question. The average current, $\boldsymbol{j}'$ and the associated average fields will be essentially constant over the unit cell, but the actual current is of course concentrated on the wires. We make a further approximation that instead of the current in each wire being surrounded by a square cell of neutralizing averaged current we redistribute this current uniformly over a circle of the same area. A valid assumption since the average fields can also be supported from the redistributed uniform current (i.e. which is equal to $\boldsymbol{j}'$). This assumption makes the local field easy to calculate since it consists of only the field of the central current and its neutralizing cloud.

If the wires are joined at the nodes so that the charge is equally distributed between the x, y, z wires, the deviation from the average electric field calculated at the surface of an x-wire is:

$$\Delta E_x = \left[Cq_x - \frac{k_0^2 j_{0x}}{4k_0}\right]\sqrt{\frac{\mu_0}{\varepsilon_0}}\mathrm{i}\frac{2}{\pi}\ln\left(\frac{a}{r_0\sqrt{\pi}}\right)\mathrm{e}^{\mathrm{i}q_x x - \mathrm{i}\omega t} \tag{15}$$

where we have borrowed the expression from [9]. The first term in square brackets is due to the charge accumulation on the wires,

$$C = \frac{\boldsymbol{q}\cdot\boldsymbol{j}_0}{12k_0}. \tag{16}$$

The second term is due to the current working against the inductance of the wires. Requiring that the field at the surface of the wire is zero,

$$\left[k_0^2 j_{0x} - q_x\boldsymbol{q}\cdot\boldsymbol{j}_0\right]\frac{1}{(q^2-k_0^2)} + \frac{k_0^2 j_{0x}}{k_\mathrm{p}^2} - Cq_x\frac{4k_0}{k_\mathrm{p}^2} = 0 \tag{17}$$

where,

$$k_\mathrm{p}^2 = \frac{2\pi}{a^2\ln\left(\frac{a}{r\sqrt{\pi}}\right)} \tag{18}$$

is the wavevector associated with the plasma frequency in (3). A more accurate approach for the plasma wavevector, accounting for the contributions from the neighbouring wires and the lattice geometry is discussed by Belov *et al* [10, 11].

For the two transverse modes $\boldsymbol{q}_\mathbf{T}\cdot\boldsymbol{j}_0 = 0$ and hence from (17),

$$k_0^2 = q_\mathrm{T}^2 + k_\mathrm{p}^2 \Rightarrow \omega = c_0\sqrt{q_\mathrm{T}^2 + k_\mathrm{p}^2}. \tag{19}$$

On the other hand the longitudinal solution corresponds to $\boldsymbol{q}_\boldsymbol{L}\times\boldsymbol{j}_0 = 0$ and hence from (17)

$$\boldsymbol{q}\cdot\boldsymbol{j}_0\left[k_0^2 - q_\mathrm{L}^2\right]\frac{1}{(q_\mathrm{L}^2-k_0^2)} + \frac{k_0^2\boldsymbol{q}\cdot\boldsymbol{j}_0}{k_\mathrm{p}^2} - Cq_\mathrm{L}^2\frac{4k_0}{k_\mathrm{p}^2} = 0. \tag{20}$$

The last term in (20) originates from the charge on the wires and if we neglect its effect, $C = 0$, then, (20) gives,

$$k_0^2 = k_\mathrm{p}^2 \Rightarrow \omega = c_0 k_\mathrm{p} \tag{21}$$

which is the ideal dispersionless longitudinal mode we should like to have. However including the corrections for charging gives,

$$k_0^2 = q_\mathrm{L}^2/3 + k_\mathrm{p}^2 \Rightarrow \omega = c_0\sqrt{q_\mathrm{L}^2/3 + k_\mathrm{p}^2}. \tag{22}$$

Note that the longitudinal and transverse plasma frequencies coincide as $q \to 0$ as required. Figure 1 shows the dispersion of the longitudinal and the transverse modes for $q \to 0$.

However, one may be concerned about the skin effect on the wires and its impact on the above dispersion equations for the wire mesh. The skin effect is determined by the penetration depth of the wave in the conducting wires (i.e. skin depth $\delta = \sqrt{\frac{2}{\mu\sigma\omega}}$, where μ and σ are the permeability and the conductivity of the wires respectively and ω is the frequency of the oscillating field). In this paper, all calculations and

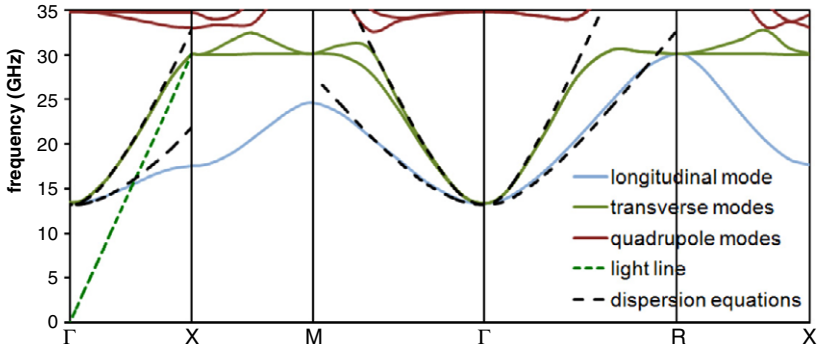

Figure 3. The band structure for $r{:}a = 0.01{:}1$ (wire's radius):(lattice constant) (where $\Gamma(0, 0, 0)$, $X(0, 0, \pi/a)$, $M(0, \pi/a, \pi/a)$, $R(\pi/a, \pi/a, \pi/a)$). The black dashed lines are the plots of (19) and (22) for the transverse and the longitudinal modes, respectively.

simulations were performed for perfectly conducting wires (i.e. infinite conductivity and no losses for the wires), and consequently δ is negligible, which means that the current is constrained to flow on the surface of the wires. This is also valid for good conductors in the microwave spectrum, where the skin depth is negligibly small. More generally, for thin wires with $r_0 \ll a$ and skin depth smaller than the radius of the wires (i.e. $\delta < r_0$), the dispersion behaviour of a wire metamaterial is independent of the skin effect and the plasma frequency (ω_p) depends only on the crystal structure (r_0 and a), as proven by [12] and [13], and is given by $\omega_p = ck_p$ (where k_p is given by (18)).

We have shown in this section that, although wire structures support transverse modes consistent with the plasmon model of dielectric response, they also support dispersive longitudinal modes making their response to external radiation more complex than a simple plasma. In some situations this is a useful property but for the most part metamaterial structures are required to simulate a local dielectric response with dispersionless longitudinal modes. We shall show that dispersion can be minimized by targeting the capacitance of the wires, or alternatively increasing their inductance so that the capacitative impedance can be neglected.

2.1. Permittivity tensors

Causality requires that all materials are dispersive [11]. Usually, the dispersive behaviour of materials can be effectively described using just the local model for the permittivity and permeability tensors, and the non-local model is considered as a small effect meaningful only in the large wavevector limit. However, it is well known that spatial dispersion exist in a 2D array of wires (i.e. a parallel-wire structure), even in the large wavelength limit [11]. Similarly, spatial dispersion is a significant effect in a 3D wire-mesh structure for the longitudinal mode, implying the need for a non-local model to homogenize the wire mesh. On the other hand, for the transverse mode no charge is accumulated on the wires, and therefore a local model can be used.

The local transverse permittivity element is given by:

$$\varepsilon_T = \varepsilon_0 \left(1 - \frac{k_p^2}{k_0^2}\right) \tag{23}$$

which depends just on the frequency of the radiation wave, and the longitudinal non-local permittivity element is given by:

$$\varepsilon_L = \varepsilon_0 \left(\frac{q^2 - 3k_0^2 + 3k_p^2}{q^2 - 3k_0^2}\right) = \varepsilon_0 \left(1 - \frac{3k_p^2}{3k_0^2 - q^2}\right) \tag{24}$$

which depends on both the frequency and the spatial components of the wavevector (analytical derivation is shown in appendix A). Note that the zeros of (24) give the dispersion equation for the longitudinal mode. Therefore, two different permittivity tensors are needed, depending on the wave's polarization.

2.2. Reflection coefficients

The difference between the local and the non-local models can be easily observed by calculating the reflection coefficients for each model. Consider a P-polarized wave[1] incident to a semi-infinite slab of a wire-mesh medium. Then, the non-local reflection coefficient is given by:

$$R_{non-loc} = \frac{q_z q_{Lz}(k_0^2 - k_p^2) - \left[q_{Tz} q_{Lz} k_0^2 + q_x^2 k_p^2\right]}{q_z q_{Lz}(k_0^2 - k_p^2) + \left[q_{Tz} q_{Lz} k_0^2 + q_x^2 k_p^2\right]} \tag{25}$$

where $q_{Lz}^2 = 3(k_0^2 - k_p^2) - (q_{Lx}^2 + q_{Ly}^2)$ is the z-axis component of the longitudinal wavevector and $q_{Tz}^2 = k_0^2 - k_p^2 - (q_{Tx}^2 + q_{Ty}^2)$ is the z-axis component of the transverse wavevector. Derivation of equation (25) can be seen in appendix B. The reflection coefficient can be reduced to the local model by considering the limit of $q_{Lz} \to \infty$:

$$R_{loc} = \lim_{q_{Lz} \to \infty} R_{non-loc} = \frac{q_z \varepsilon(\omega) - q_{Tz}}{q_z \varepsilon(\omega) + q_{Tz}} \tag{26}$$

where $\varepsilon(\omega) = \varepsilon_T(\omega) = 1 - \frac{k_p^2}{k_0^2}$. Equations (25) and (26) predict different results for the reflection coefficient, where the local model falsely ignores the propagation of the longitudinal mode in the wire medium.

[1] A P-polarized wave has the electric field in the plane of incidence. The plane of incidence is defined by the direction of propagation (i.e. the wavevector) and the normal of the reflecting surface. Sometimes the P-polarized wave are referred to as transverse-magnetic (TM) waves. S-polarized waves have the electric field perpendicular to the plane of incidence and are often referred to as transverse-electric (TE) waves.

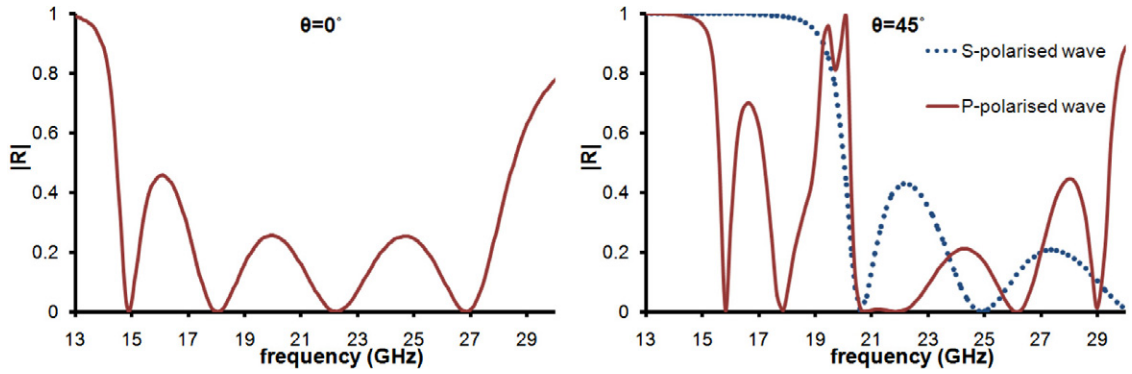

Figure 4. The modulus of the reflection coefficient for the wire-mesh metamaterials for various angles of incidence. S-polarized wave (i.e. dotted line) and P-polarized wave (i.e. full line): left figure—$\theta = 0°$, right figure—$\theta = 45°$.

Using CST Microwave studio, the band structure of the wire mesh ($r/a = 0.01$) shown in figure 2 and the reflection coefficient for a finite slab of five unit cells (i.e. $d = 5a$ and $r/a = 0.01$) were calculated. The results are shown in figures 3 and 4 respectively. In figure 3, a doubly degenerate transverse mode is shown and the dispersion of the longitudinal mode can be seen, which is clearly significant. Also, the dispersion equations shown in (19) and (22) for the transverse and the longitudinal modes respectively, are plotted with black dashed lines, and their agreement with the simulation results is significant (especially for $q \to 0$). Also, two degenerate quadrupole modes, not predicted in theory, arise (at ~35 GHz), due to the orthogonal structure of the wire mesh. It is worth mentioning that there are just two independent quadrupole modes.

In figure 4, the reflection coefficient is shown for wires in a loss-free hosting medium. The longitudinal mode is excited for the P-polarized wave and for non-normal angles of incidence ($\theta \neq 0$). The contribution of the longitudinal mode in the interference pattern is significant and the effect of spatial dispersion clear. Since the longitudinal mode is not excited for the S-polarized wave, a comparison between the interference pattern of the two waves can indicate the effect of spatial dispersion on the wire system.

3. New structures

In this paper, new wire structures are proposed, that manage to eliminate the effect of spatial dispersion for the wire mesh. As mentioned before, spatial dispersion arises from the periodic charge accumulation in the wires. There are two main ways to avoid spatial dispersion for the wire-mesh metamaterial. Either increase the capacitance of the system, by attaching conducting structures on the wires (i.e. conducting plates, spheres, cubes, cylinders etc.), or increase the inductance of the system, by coating the wires with a magnetic material.

However, by changing the structure of the wire mesh, the effective permittivity elements change as well. In order to model these various complex wire structures and calculate their dependence on spatial dispersion, the method described by Shapiro *et al* [14] was used. He modelled the wire-mesh structure as a 'cubic crystal with spatial dispersion' and expressed the permittivity tensors with respect to the calculated band structure. This method can be expanded and used for modelling the permittivity tensors for any wire structure, provided that its band structure is given. Therefore, the permittivity element describing the behaviour of any wire structure to incident radiation along one of the wires (e.g. z-wire) are given by:

$$\varepsilon_{\mathrm{T}} = \beta\left(1 - \frac{k_{\mathrm{p}}^2}{k_0^2}\right) + \alpha_2 \frac{q_z^2}{k_0^2}$$
$$\varepsilon_{\mathrm{L}} = \beta\left(1 - \frac{k_{\mathrm{p}}^2}{k_0^2}\right) + \alpha_1 \frac{q_z^2}{k_0^2} \tag{27}$$

where β is a coefficient accounting for the polarization of the attached structures on the wires ($\beta = 1$ for just the wire mesh-no structures) and α_1, α_2 are frequency dependent spatial dispersion coefficients, determining the dependence of the permittivity tensor on the spatial component of the wavevector. The coefficients α_1 and α_2 can be determined by fitting the calculated band structures to equation (28), for the small wavevector limit (i.e. $q \to 0$) [14]:

$$\omega^2 = \omega_{\mathrm{p}}^2 + Aq^2c^2 \tag{28}$$

where A is a constant. For the longitudinal mode: $A = -\alpha_1/\beta$ and for the transverse modes: $A = (1 - \alpha_2)/\beta$. α_1 and α_2 also depend on the dimensions of the lattice and the wires.

As an example, consider the wire-mesh structure shown in figure 2 (with $r/a = 0.01$). From its band structure (i.e. Figure 3) the spatial dispersion coefficients have values: $\alpha_1 = -0.307$ and $\alpha_2 = 0.035$. This means that the spatial dispersion for the transverse mode is determined by α_2, which is negligible for $r \ll a$ and therefore the permittivity tensor is given by (23). On the other hand, the spatial dependence of the longitudinal permittivity tensor will be dominated by α_1, which is significant for the wire-mesh structure, even for $r \ll a$. Therefore, the new structures should have negligible values for both α_1 and α_2.

3.1. Increasing the capacitance of the structure

As mentioned before, a way to avoid spatial dispersion in the wire mesh is to increase its capacitance by attaching

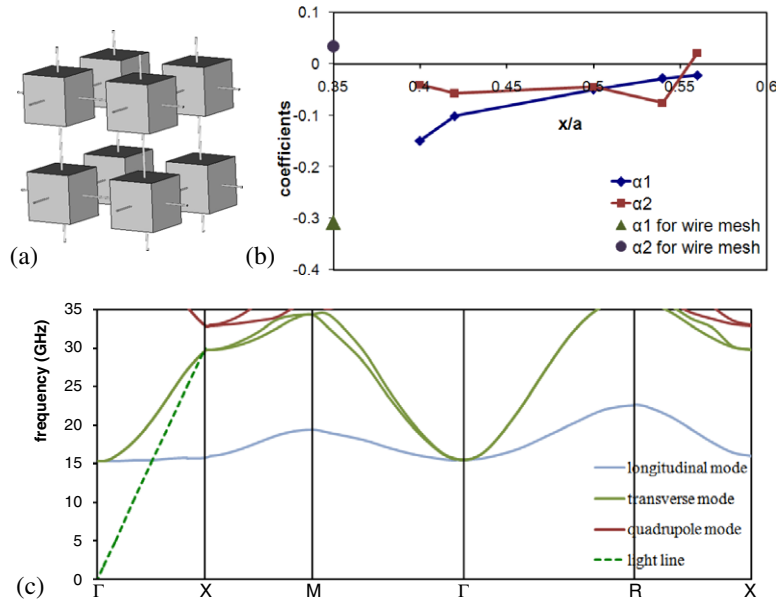

Figure 5. (a) The wire mesh with cubes attached at the joints, (b) α_1 and α_2 coefficients are plotted against the dimensions of the cube, where x is the side of the cube, a is the lattice constant and $r/a = 0.01$ for all the calculations, (c) the band structure for $r{:}x{:}a = 0.01{:}0.5{:}1$ (wire's radius):(side of cube):(lattice constant) (where $\Gamma(0, 0, 0)$, $X(0, 0, \pi/a)$, $M(0, \pi/a, \pi/a)$, $R(\pi/a, \pi/a, \pi/a)$).

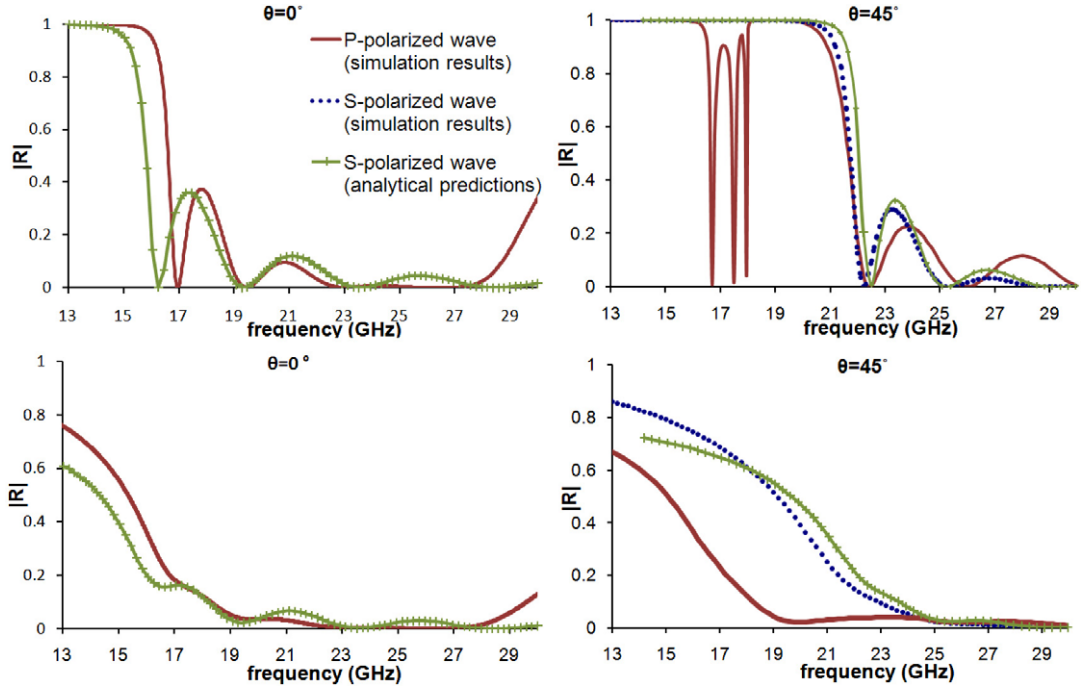

Figure 6. The modulus of the reflection coefficient for the structure shown in figure 5. Both the S-polarized (dashed line) and the P-polarized waves (full line) are shown for various angles of incidence. Also, the reflection coefficient was calculated for both a loss-free hosting medium (top graphs) and a lossy medium in order to simulate a real material (bottom graphs).

conducting structures on the wires. Therefore, the charge accumulated on the wires of the wire mesh, causing spatial dispersion, will now be distributed on the attached conducting structures leaving the plasma-like behaviour of the wires unaffected. Various structures have been tested and all showed significant reduction of spatial dispersion. However, the structures with the highest efficiency in avoiding spatial dispersion are shown in figures 5(a) and 7(a). CST Microwave Studio was used to perform finite integrations of Maxwell's equations and calculate the band structures and the reflection coefficients of the following structures.

For the structure shown in figure 5, cubes were introduced at the joints of the wires. However, this shortens the wires, causing the plasma frequency to increase (i.e. $m_{\text{eff}}^{\text{wires}} > m_{\text{eff}}^{\text{cube+wires}}$). The effect of spatial dispersion on the longitudinal mode varies with the dimensions of the cube, as shown in

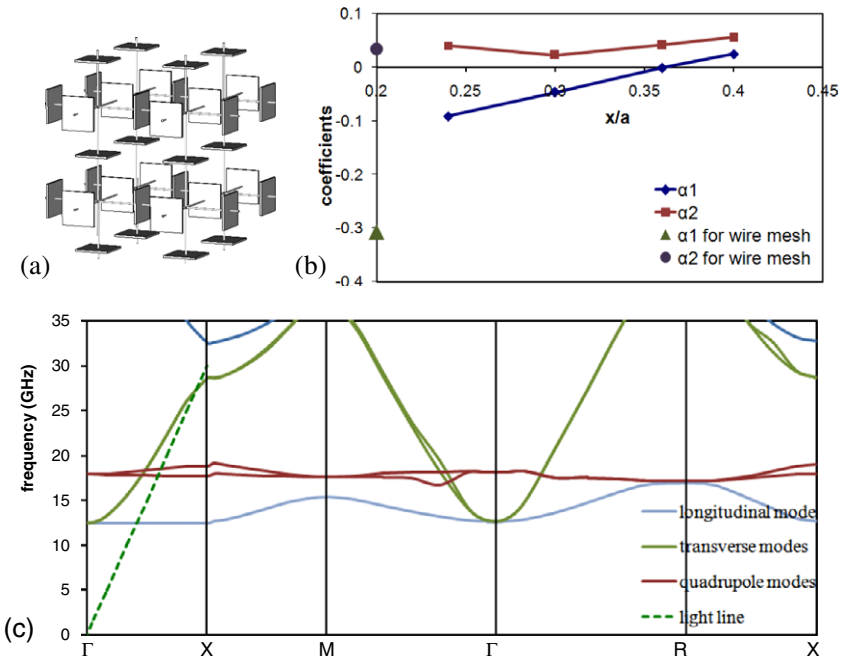

Figure 7. (a) The wire mesh with plates at the mid-points between the joints, (b) α_1 and α_2 coefficients are plotted against the dimensions of the plates, where x is the side of the square plates, a is the lattice constant, (c) the band structure for $r{:}x{:}a = 0.01{:}0.36{:}1$ (wire's radius):(side of square plate):(lattice constant) (where $\Gamma(0, 0, 0)$, $X(0, 0, \pi/a)$, $M(0, \pi/a, \pi/a)$, $R(\pi/a, \pi/a, \pi/a)$).

figure 5 expressed with α_1 and α_2 coefficients. Finally, the two degenerate quadrupole modes, appear at much higher frequencies (∼49 GHz).

Another, more efficient way, to increase the capacitance of the wire mesh, is to introduce thin square plates at the mid-points between the joints of the wires, as shown in figure 7(a). The thin plates have the advantage of dramatically increasing the capacitance of the system, without affecting the plasma behaviour of the wire medium. From figures 7(b) and (c), it can be seen that the dispersion of the longitudinal mode is dramatically reduced, indicating that the longitudinal permittivity element does not depend on the spatial components of the wavevector. The effect of spatial dispersion for the longitudinal mode depends on the dimensions of the plates introduced on the structures (see figure 7(b)). Finally, the two quadrupole degenerate modes are seen at lower frequencies (∼25 GHz).These two modes are also flat (i.e. the group velocity is zero: $\frac{d\omega}{dq} = 0$), and therefore they do not propagate in the medium either, but they create additional surface plasmons at the interface between air and the wire medium.

For both structures (shown in figures 5(a) and 7(a)), the reflection coefficient was calculated for a finite slab of five unit cells (i.e. $d = 5$ N) and the results are plotted in figures 6 and 8 respectively. Simulations were performed for perfectly conducting wires in free space, where losses were ignored and in a slightly lossy dielectric hosting medium (in order to simulate a real hosting material). The lossy hosting medium has a permittivity tensor of the form $\varepsilon = \varepsilon' + i\varepsilon'' = \varepsilon_0[1 + i\sigma/(\omega\varepsilon_0)]$, where σ and ω are the conductivity of the hosting medium and the frequency of the wave respectively and real permittivity $\varepsilon' = 1$. CST accepts values for the conductivity of the hosting medium and it was chosen to be $\sigma = 0.111$ S m^{-1}, giving an imaginary permittivity $\varepsilon'' \approx 0.1$ at 20 GHz.

The reflection coefficients are plotted in figures 6 and 8 for the structures shown in figures 5(a) and 7(a) respectively. The longitudinal mode is excited for the P-polarized wave and for non-normal angles of incidence, giving sharp resonances for a loss-free hosting medium. However, for a real system, that is slightly lossy, these resonances are absorbed, meaning that the flat modes cannot propagate in the medium. These modes are now creating surface plasmons at the interface between the wire medium and a dielectric. Therefore, these wire structures can be effectively described by one local permittivity tensor each.

For both structures, the two spatial dispersion coefficients (α_1, α_2) are negligibly small ($\alpha_1 = -0.049$, $\alpha_2 = -0.045$ and $\beta = 1.24$ for the $x/a = 0.5$ for the structure in figure 5(a) and $\alpha_1 \to 0$, $\alpha_2 = 0.04$ and $\beta = 1.04$ for the $x/a = 0.36$ for the structure in figure 7(a)), and therefore the loss-free wire structure can be modelled with one local permittivity tensor, given by:

$$\varepsilon = \beta\left(1 - \frac{\omega_p^2}{\omega_0^2}\right) \tag{29}$$

and when losses are present, the general form of the Drude model applies where:

$$\varepsilon = \varepsilon_1 - \frac{\Omega^2}{\omega(\omega + i\gamma)} \tag{30}$$

where $\Omega = \omega_p\sqrt{\varepsilon_1}$, γ represents the resistivity losses in the system, and ε_1 is a constant. Therefore, for a finite slab, the scattering parameters for a P- and a S-polarized wave can be calculated according to Pendry's work in [15]. Note that for

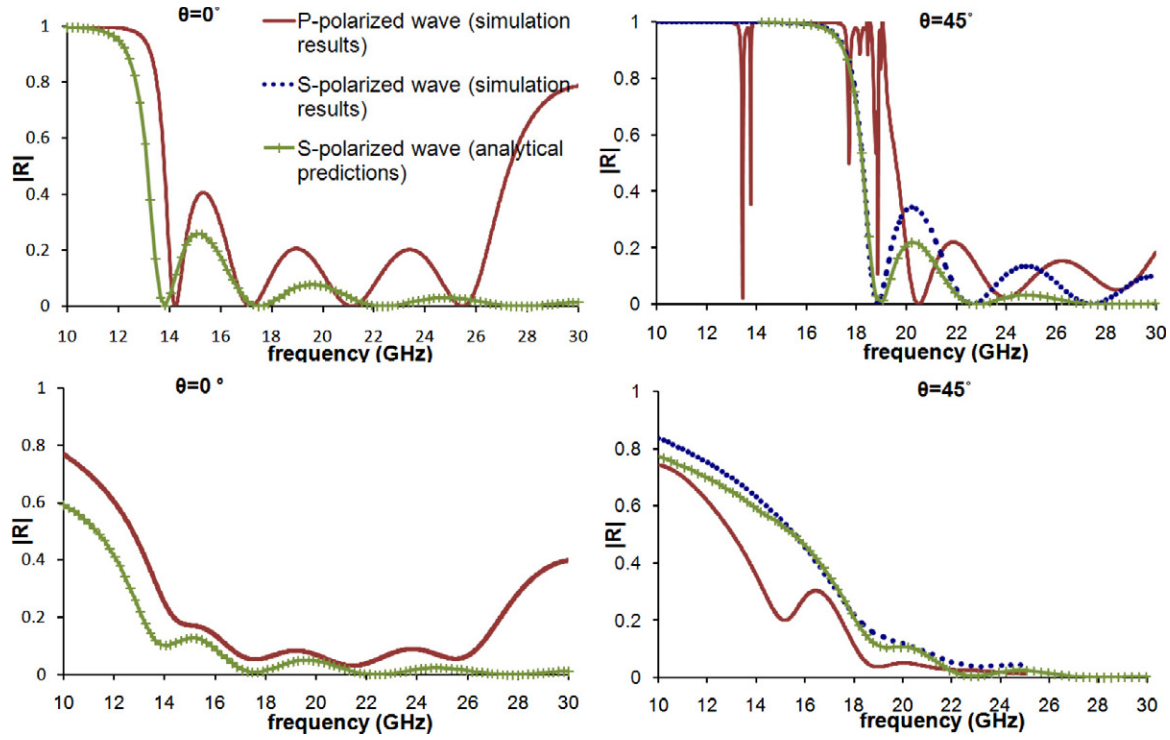

Figure 8. The modulus of the reflection coefficient for the structure shown in figure 7. Both the S-polarized (dashed line) and the P-polarized waves (full line) are shown for various angles of incidence. Also, the reflection coefficient was calculated for both a loss-free hosting medium (top graphs) and a lossy medium in order to simulate a real material (bottom graphs).

normal incidence, $q_z' = \sqrt{\varepsilon} q_z$ for the S-polarized wave and $q_z' = q_z$ for the P-polarized wave.

$$R_{\mathrm{P}} = \frac{\varepsilon - 1}{\varepsilon + 1} + \frac{4\varepsilon(1-\varepsilon)\exp(\mathrm{i}q_z d)}{(\varepsilon+1)\left[(\varepsilon+1)^2 - (1-\varepsilon)^2\exp(2\mathrm{i}q_z d)\right]}$$

$$R_{\mathrm{S}} = \frac{\sqrt{\varepsilon} - 1}{\sqrt{\varepsilon} + 1} \tag{31}$$

$$+ \frac{4\sqrt{\varepsilon}(\sqrt{\varepsilon}-1)\exp(\mathrm{i}q_z' d)}{(\sqrt{\varepsilon}+1)\left[(\sqrt{\varepsilon}+1)^2 - (\sqrt{\varepsilon}-1)^2\exp(2\mathrm{i}q_z' d)\right]}$$

where q_z' is the component of the wavevector inside the medium, q_z is the component of the wavevector outside the medium, $d = Na$ is the length of the finite slab examined, N is the number of unit cells used and a the lattice constant. In figures 6 and 8, the simulation calculations for normal incidence of the reflection coefficient is plotted with the analytical predictions from (31) for the two structures. It is clear that there is significant agreement. However, at high frequencies the agreement fails due to the band gap of the transverse mode at ∼30 GHz, which is not predicted from (31). Also, for higher frequencies, the wavelength becomes small enough for internal scattering within the structure to take place, an effect not described by (31), since it assumes a slab of homogeneous medium.

3.2. Increasing the inductance of the structure

Another way to minimize spatial dispersion in a wire system is to increase its inductance, by coating the wires with a magnetic material as shown in figure 9(a). This material enhances the magnetic and consequently the electric field associated with the plasma behaviour of the structure, but leaves the local electrostatic part (i.e. accumulated charge) unaffected. Therefore, the relative importance of the charge accumulation in the wires is reduced.

From figures 9(b) and (c), it can be seen that the dispersion of the longitudinal mode is decreased significantly. The α_1 and α_2 coefficients take negligibly small values and therefore the spatial dependence of the permittivity element can be ignored. Also, note that $\beta = 1$, since no conducting structures were attached on the wires. Also, note that the plasma frequency is reduced, since the self-inductance effects causing m_{eff} are enhanced (i.e. $m_{\mathrm{eff}}^{\mathrm{magn-coat}} > m_{\mathrm{eff}}^{\mathrm{wire-mesh}}$).

For the structure shown in figure 9(a), the reflection coefficient was calculated for a finite slab of five unit cells (i.e. $d = 5a$). Again, simulations were performed for perfectly conducting wires in free space, where losses were ignored and in a slightly lossy dielectric hosting medium (in order to simulate a real hosting material). The lossy hosting medium has a permittivity tensor of the form $\varepsilon = \varepsilon' + \mathrm{i}\varepsilon'' = \varepsilon_0[1 + \mathrm{i}\sigma/(\omega\varepsilon_0)]$, with real permittivity $\varepsilon' = 1$. CST accepts values for the conductivity and it was chosen to be $\sigma = 0.083$ S m^{-1}, giving an imaginary permittivity $\varepsilon'' \approx 0.1$ at 15 GHz.

In figure 10, the reflection coefficient is plotted for both the loss-free and the lossy hosting dielectric. The longitudinal and the quadrupole modes are excited for a P-polarized wave and non-normal angles of incidence, and they can be seen as sharp resonances for the loss-free hosting medium. However, these resonances are absorbed when the hosting medium is slightly lossy, as all real

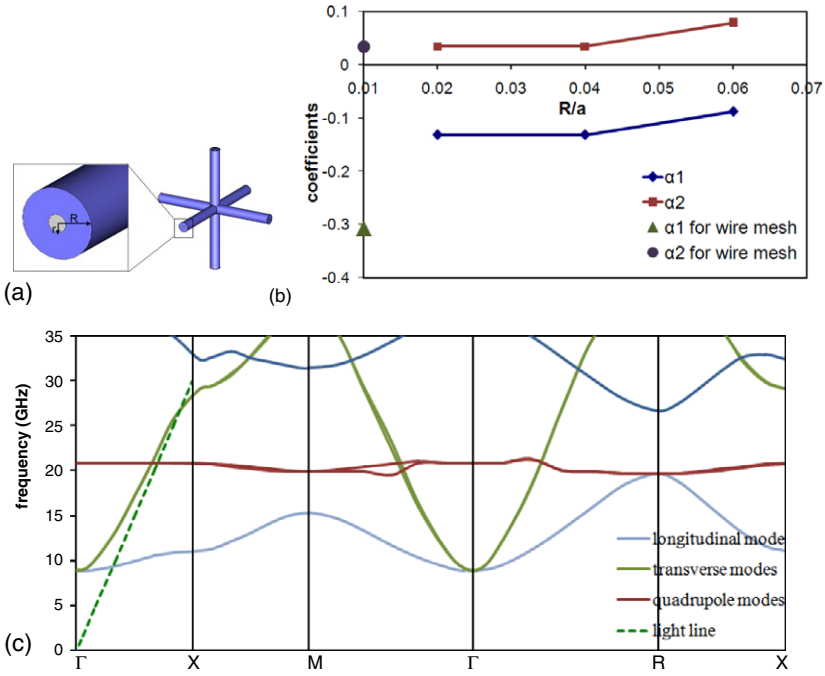

Figure 9. (a) The magnetically ($\mu = 5$) coated wire-mesh metamaterial, (b) α_1 and α_2 coefficients plotted against the dimensions of the coating material, where R is the outer radius of the coating material, a is the lattice constant and for all calculations $r/a = 0.01$, (c) the band structure for $r{:}R{:}a = 0.01{:}0.04{:}1$ (wire's radius):(outer radius of the coating material):(lattice constant), (where $\Gamma(0, 0, 0)$, $X(0, 0, \pi/a)$, $M(0, \pi/a, \pi/a)$, $R(\pi/a, \pi/a, \pi/a)$).

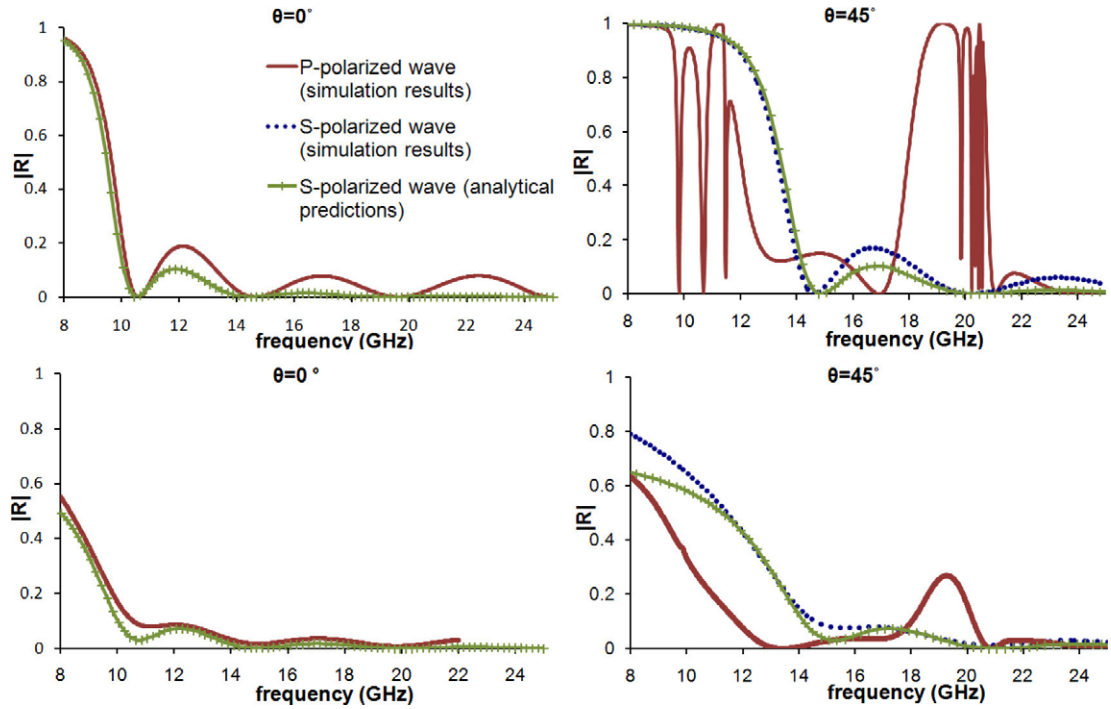

Figure 10. The modulus of the reflection coefficient for the structure shown in figure 9. Both the S-polarized (blue dashed line) and the P-polarized waves (pink full line) are shown for various angles of incidence. Also, the reflection coefficient was calculated for both a loss-free hosting medium (top graphs) and a lossy medium in order to simulate a real material (bottom graphs).

materials are. Then, it is clear that the longitudinal and quadrupole modes do not propagate in a real system, but only the transverse mode propagates, concluding that the new wire metamaterial can be homogenized by one local permittivity tensor given by (23). Therefore, by substituting this permittivity tensor in (31), analytical predictions can be derived for the reflection coefficient, which is plotted in figure 10. It is clear that there is significant agreement between the analytical predictions and the simulation calculations.

4. Conclusions

It is known, that a wire-mesh structure has 3D-plasma-like properties and is used as a negative permittivity metamaterial. However, the properties of this artificial plasma are strongly modified by spatial dispersion, which arises from periodic charge accumulation in the wires for longitudinal waves, preventing the homogenization of the wire medium by one local permittivity tensor. Spatial dispersion can be avoided by attaching conducting structures on the wires and therefore increasing the capacitance of the wire system or by coating the wires with a magnetic material, which increases the inductance of the wire system.

By eliminating spatial dispersion in wire structures, the longitudinal mode becomes dispersion free and hence is excluded form propagating in the wire medium. Therefore, the longitudinal mode (and the quadrupole modes, who are also dispersion free) create surface plasmons at a wire-medium/vacuum interface. Finally, since the transverse mode is the only mode propagating in the medium, these new wire structures can be homogenized by one effective local permittivity tensor, identical to the permittivity tensor for the transverse mode.

Appendix A. Derivation of the non-local permittivity tensor for the wire-mesh structure

The mean electric field in the wire-mesh structure induced by an electromagnetic wave is given by (14) and the deviation from the average electric field at the surface of an x-wire by (15).

Now, by adding a new source term (i.e. $\boldsymbol{J}_0$), the electric field at the wires (which should always be zero, since perfect electric conducting wires are considered) is given by:

$$E_x - \Delta E_x = \frac{\mathrm{i}\omega\mu_0(j_{0x}+J_{0x}) - \mathrm{i}q_x\frac{(j_0+J_0)\cdot q}{\varepsilon_0\omega}}{(q^2-k_0^2)a^2} - \sqrt{\frac{\mu_0}{\varepsilon_0}}\frac{\mathrm{i}}{k_\mathrm{p}^2 a^2} \times \left(\frac{q_x \boldsymbol{q}\cdot\boldsymbol{j}_0}{3k_0} - \frac{k_0^2 j_{0x}}{k_0}\right) = 0 \tag{A.1}$$

$$\therefore \frac{\mathrm{i}}{a^2 k_0}\sqrt{\frac{\mu_0}{\varepsilon_0}}\left[\frac{(k_0^2-q_x^2)(J_{0x}+j_{0x})}{(q^2-k_0^2)} - \frac{(q_x^2-3k_0^2)j_{0x}}{3k_\mathrm{p}^2}\right] = 0. \tag{A.2}$$

If you assume propagation along the x-axis, then for the longitudinal mode, $\boldsymbol{q} = q_x\hat{\boldsymbol{x}}$, $\boldsymbol{J}_0 = J_{0x}\boldsymbol{q}$ and $\boldsymbol{j}_0 = j_{0x}\boldsymbol{q}$ are valid, which leads to a relation between the two sources:

$$J_{0x} = -j_{0x}\left(\frac{q_x^2-3k_0^2+3k_\mathrm{p}^2}{3k_\mathrm{p}^2}\right) = -j_{0x} - j_{0x}\left(\frac{q_x^2-3k_0^2}{3k_\mathrm{p}^2}\right). \tag{A.3}$$

Therefore, using Maxwell equations, the permittivity tensor for the longitudinal mode is given by:

$$\varepsilon_\mathrm{L} = \frac{\nabla\boldsymbol{D}}{\nabla\boldsymbol{E}} = \frac{J_{0x}}{J_{0x}+j_{0x}} = \varepsilon_0\left(1-\frac{3k_\mathrm{p}^2}{3k_0^2-q_z^2}\right). \tag{A.4}$$

Appendix B. Derivation of the non-local reflection coefficient for a semi-infinite slab of the wire-mesh medium

Consider a p-polarized wave incident on a semi-infinite slab of the system shown in figure 2.

Appendix B.1. Reflected fields

The incident and reflected magnetic field is given by:

$$\boldsymbol{H} = \hat{\boldsymbol{y}}H_0\exp(\mathrm{i}q_x x + \mathrm{i}q_y y - \mathrm{i}\omega t)\left(\mathrm{e}^{\mathrm{i}q_z z} + R\mathrm{e}^{-\mathrm{i}q_z z}\right) \tag{B.1}$$

and the electric field can be derived by Maxwell equation and is given by:

$$\frac{\partial D}{\partial t} = \nabla\times\boldsymbol{H} \Rightarrow \boldsymbol{E} = -\frac{1}{\mathrm{i}\varepsilon_0\omega}\nabla\times\boldsymbol{H} \tag{B.2}$$

$$\boldsymbol{E} = H_0\exp(\mathrm{i}q_x x + \mathrm{i}q_y y - \mathrm{i}\omega t)\left[\frac{q_z\hat{\boldsymbol{x}} - q_x\hat{\boldsymbol{z}}}{\varepsilon_0\omega}\mathrm{e}^{\mathrm{i}q_z z} - \frac{q_z\hat{\boldsymbol{x}} + q_x\hat{\boldsymbol{z}}}{\varepsilon_0\omega}R\mathrm{e}^{-\mathrm{i}q_z z}\right]. \tag{B.3}$$

Appendix B.2. Transmitted fields

Consider the electric and magnetic fields inside the metamaterial (i.e. equations (13) and (14)).

$$\boldsymbol{B} = \frac{\mathrm{i}\mu_0\boldsymbol{q}\times\boldsymbol{j}_0}{(q^2-k_0^2)a^2}\exp(\mathrm{i}q_x x + \mathrm{i}q_y y + \mathrm{i}q_z z - \mathrm{i}\omega t) \tag{B.4}$$

$$\boldsymbol{E} = \left[\mathrm{i}\omega\mu_0\boldsymbol{j}_0 - \mathrm{i}\boldsymbol{q}\frac{\boldsymbol{j}_0\cdot\boldsymbol{q}}{\varepsilon\omega}\right]\frac{1}{(q^2-k_0^2)a^2} \times \exp(\mathrm{i}q_x x + \mathrm{i}q_y y + \mathrm{i}q_z z - \mathrm{i}\omega t). \tag{B.5}$$

There are two modes that propagate in the wire-mesh medium: the transverse and the longitudinal mode.

For the longitudinal mode, the dispersion equation is given by: $q^2 = 3(k_0^2 - k_\mathrm{p}^2)$, and the current induced in the wires due to the longitudinal mode is $\boldsymbol{j_L} = J_\mathrm{L}H_0\boldsymbol{q_L} = J_\mathrm{L}H_0(q_\mathrm{L}\hat{\boldsymbol{x}}+q_z\hat{\boldsymbol{z}})$. Therefore, the magnetic field associated with the longitudinal mode is:

$$B_L = \frac{\mathrm{i}\mu_0\boldsymbol{q_\mathrm{L}}\times\boldsymbol{j_L}}{(q^2-k_0^2)a^2}\exp(\mathrm{i}q_x x + \mathrm{i}q_y y + \mathrm{i}q_z z - \mathrm{i}\omega t) = 0 \tag{B.6}$$

and is equal to zero, since the wavevector is parallel to the electric field producing the current and therefore the current in the wires is parallel to the wavevector (i.e. their cross product is zero). Now, the electric field due to the longitudinal mode is given by:

$$\boldsymbol{E_L} = \frac{\mathrm{i}\omega\mu_0 J_\mathrm{L}H_0(q_\mathrm{L}\hat{\boldsymbol{x}} + q_z\hat{\boldsymbol{z}}) - \mathrm{i}\frac{J_\mathrm{L}H_0 q_\mathrm{L}^2}{\varepsilon\omega}\boldsymbol{q_L}}{(q^2-k_0^2)a^2} \times \exp(\mathrm{i}q_x x + \mathrm{i}q_y y + \mathrm{i}q_z z - \mathrm{i}\omega t). \tag{B.7}$$

Consider for simplicity, the electric field tangential to the surface (i.e. in the x–y plane), and since the longitudinal wavevector is always parallel to the electric field (i.e. $\boldsymbol{q_L} = q_x\hat{\boldsymbol{x}}$), the electric field associated with the longitudinal mode at surface $z = 0$ is given by:

$$E_L^x = -\frac{\mathrm{i}\omega\mu_0 J_\mathrm{L}H_0 q_x}{k_0^2 a^2}\exp(\mathrm{i}q_x x + \mathrm{i}q_y y + \mathrm{i}q_z z - \mathrm{i}\omega t). \tag{B.8}$$

For the transverse mode, the dispersion equation is given by: $q^2 = k_0^2 - k_p^2$, and the current induced in the wires due to the transverse mode is $\boldsymbol{j_T} = J_T H_0 \boldsymbol{q_T} = J_T H_0 (q_T \hat{\boldsymbol{x}} + q_x \hat{\boldsymbol{z}})$. Therefore, the magnetic field due to the transverse mode can be calculated using equation (B.4) and by applying the above conditions:

$$\boldsymbol{H_T} = -\frac{\mathrm{i} J_T H_0 (k_0^2 - k_p^2)\hat{\boldsymbol{y}}}{k_p^2 a^2} \exp(\mathrm{i}q_x x + \mathrm{i}q_y y + \mathrm{i}q_z z - \mathrm{i}\omega t) \tag{B.9}$$

and the electric field tangential to the surface (i.e. on the x–y plane) is given by:

$$E_T^x = -\frac{\mathrm{i}\omega\mu_0 J_T H_0 q_{Tz}}{k_p^2 a^2} \exp(\mathrm{i}q_x x + \mathrm{i}q_y y + \mathrm{i}q_z z - \mathrm{i}\omega t). \tag{B.10}$$

It is required that the current at the surface to be zero. Therefore, the currents induced from the two modes should add to zero: $\boldsymbol{j_T} + \boldsymbol{j_L} = -J_T H_0 \boldsymbol{q_T} + J_L H_0 \boldsymbol{q_L} = 0$ and by considering current flowing in the wires along the z-axis: $J_L = \frac{J_T q_x}{q_{Lz}}$ Hence, the total magnetic and electric fields transmitted due to both modes are:

$$H = -\frac{\mathrm{i} J_T H_0 (k_0^2 - k_p^2)}{k_p^2 a^2} \exp(\mathrm{i}q_x x + \mathrm{i}q_y y + \mathrm{i}q_z z - \mathrm{i}\omega t) \tag{B.11}$$

$$E_x = -\frac{\mathrm{i}\omega\mu_0 J_T H_0}{a^2} \left[\frac{q_x^2}{k_0^2 q_{Lz}} + \frac{q_{Tz}}{k_p^2} \right] \times \exp(\mathrm{i}q_x x + \mathrm{i}q_y y + \mathrm{i}q_z z - \mathrm{i}\omega t). \tag{B.12}$$

Appendix B.3. Reflection coefficient (R)

Now, by matching the magnetic fields at the surface ($z = 0$), the following relation is derived:

$$1 + R = -\frac{\mathrm{i} J_T (k_0^2 - k_p^2)}{k_p^2 a^2} \tag{B.13}$$

and by matching the tangential electric fields at the surface of incidence:

$$1 - R = -\frac{\mathrm{i} J_T k_0^2}{a^2 q_z} \left[\frac{q_x^2}{k_0^2 q_{Lz}} + \frac{q_{Tz}}{k_p^2} \right]. \tag{B.14}$$

Solving these two equations, the non-local reflection coefficient can be derived for a semi-infinite slab of a wire-mesh medium:

$$R = \frac{q_z q_{Lz} (k_0^2 - k_p^2) - \left[q_{Tz} q_{Lz} k_0^2 + q_x^2 k_p^2 \right]}{q_z q_{Lz} (k_0^2 - k_p^2) + \left[q_{Tz} q_{Lz} k_0^2 + q_x^2 k_p^2 \right]}. \tag{B.15}$$

References

[1] Veselago V G 1968 The electrodynamics of substances with simultaneously negative values of ε and μ *Sov. Phys.—Usp.* **10** 509

[2] Pendry J B, Holden A J, Stewart W J and Young I 1996 Extremely low frequency plasmons in metallic mesostructures *Phys. Rev. Lett.* **76** 4773–6

[3] Pendry J B, Holden A J, Robbins D J and Stewart W J 1998 Low frequency plasmons in thin-wire structures *J. Phys.: Condens. Matter* **10** 4785–809

[4] Brown J 1960 Artificial dielectrics *Prog. Dielectr.* **2** 195

[5] Rotman W 1962 Plasma simulation by artificial dielectrics and parallel-plate media *IEEE Trans. Antennas Propag.* **10** 82–95

[6] Gay-Balmaz P, Maccio C and Martin O J F 2002 Microwave arrays with plasmonic response at microwave frequencies *Appl. Phys. Lett.* **81** 2896–8

[7] Shvets G 2002 *Photonic Approach to Making a Surface Wave Accelerator* vol 647 (New York: American Institute of Physics) pp 371–82

[8] Shvets G, Sarychev A K and Shalaev V M 2003 Electromagnetic properties of three-dimensional wire arrays: photons, plasmons, and equivalent circuits *Proc. SPIE* **5218** 156

[9] Silveirinha M G and Fernandes C A 2005 Homogenization of 3d-connected and nonconnected wire metamaterial *IEEE Trans. Microw. Theory Tech.* **53** 1418–30

[10] Belov P A, Tretyakov S A and Viitanen A 2002 Dispersion and reflection properties of artificial media formed by regular lattices of ideally conducting wires *J. Electromagn. Waves Appl.* **16** 1153–70

[11] Belov P A, Marques R, Maslovski S I, Nefedov I S, Silveirinha M, Simovski C R and Tretyakov S A 2003 Strong spatial dispersion in wire media in the very large wavelength limit *Phys. Rev.* B **67** 113103

[12] Sarychev A K, McPhedram R C and Shalaev V M 2000 Electrodynamics of metal–dielectric composites and electromagnetic crystals *Phys. Rev.* B **62** 8531–9

[13] Silveirinha M G, Belov P A and Simovski C R 2007 Subwavelength imaging at infrared frequencies using an array of metallic nanorods *Phys. Rev.* B **75** 035108

[14] Shapiro M A, Shvets G, Sirigiri L R and Temkin R J 2006 Spatial dispersion in metamaterials with negative dielectric permittivity and its effect on surface waves *Opt. Lett.* **31** 2051–53

[15] Pendry J B 2000 Negative refraction makes a perfect lens *Phys. Rev. Lett.* **85** 3966–69